INSTITUTE OF PHYSICS PUBLISHING JOURNAL OF PHYSICS: CONDENSED MATTER

J. Phys.: Condens. Matter **18** (2006) S245–S252 doi:10.1088/0953-8984/18/14/S09

Spatially confined polymer chains: implications of chromatin fibre flexibility and peripheral anchoring on telomere–telomere interaction

L R Gehlen[1], A Rosa[2,5], K Klenin[3], J Langowski[3], S M Gasser[1] and K Bystricky[4,6]

[1] Friedrich Miescher Institute for Biomedical Research, 4058 Basel, Switzerland
[2] Institut de Mathématiques B, École Polytechnique Fédérale de Lausanne, 1015 Lausanne, Switzerland
[3] Division of Biophysics of Macromolecules, German Cancer Research Center (Deutsches Krebsforschungszentrum), 69120 Heidelberg, Germany
[4] Laboratoire de Biologie Moléculaire Eucaryote/IBCG, Université Paul Sabatier, 31062 Toulouse Cedex, France

E-mail: kerstin@ibcg.biotoul.fr

Received 5 October 2005
Published 24 March 2006
Online at stacks.iop.org/JPhysCM/18/S245

Abstract

We simulate the extension of spatially confined chromatin fibres modelled as polymer chains and examine the effect of the flexibility of the fibre and its degree of freedom. The developed formalism was used to analyse experimental data of telomere–telomere distances in living yeast cells in the absence of confining factors as identified by the proteins Sir4 and yKu70. Our analysis indicates that intrinsic properties of the chromatin fibre, in particular its elastic properties and flexibility, can influence the juxtaposition of the telomeric ends of chromosomes. However, measurements in intact yeast cells showed that the telomeres of chromosomes 3 and 6 come even closer together than the parameters of constraint imposed on the simulations would predict. This juxtaposition was specific to telomeres on one contiguous chromosome and overrode a tendency for separation that is imposed by anchoring.

1. Introduction

DNA is a long flexible filament that is highly compacted in the cell nucleus. The resulting chromatin fibre allows regulated access to factors of the replication, transcription and repair machineries. To understand the mechanisms of chromatin compaction and regulation, knowledge of the nanomechanical parameters and the dynamics of DNA, chromatin and

[5] Present address: Max-Planck Institut für Physik Komplexer Systeme, 01187 Dresden, Germany.
[6] Author to whom any correspondence should be addressed.

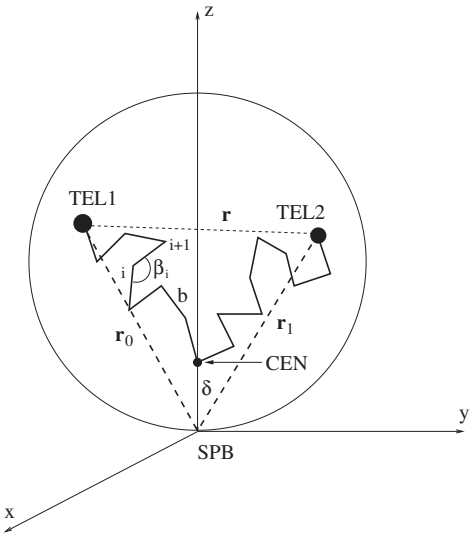

Figure 1. The chromosome was modelled as a flexible chain with bond length b. One bead representing the centromere (CEN) was fixed or elastically attached to the spindle pole body (SPB) at a distance $\delta \simeq 300$ nm [2].

chromosomes is fundamental. While numerous studies on the flexibility of the chromatin fibre exist, the influence of spatial confinement on the conformation of chromatin has only been investigated in a few cases.

Chromosome extension, location and movement can be monitored in intact yeast cells by fluorescence microscopy. In a previous study [1] using a flexible polymer model we have shown that interphase chromatin exists in a rather compact higher order conformation with a persistence length $L_p = 170$–220 nm and a mass density $c = 110$–150 bp nm^{-1}. The extension of this fibre, thus of chromosome arms, is largely influenced by nuclear geometry. Furthermore, the two ends of the same chromosome tend to interact frequently and are closer in space than telomeres of distinct chromosomes [2].

Here we used Monte Carlo simulations to determine which parameters influence the interaction of spatially confined polymer chains. We modelled the two chromosome arms connected at their centrally located centromere (CEN) which is attached to the spindle pole body (SPB) via flexible microtubules [2]. The SPB was represented by an immobile point embedded in the nuclear periphery. The nucleus of the cell was modelled as a sphere with radius $R \simeq 900$ nm; see figure 1.

2. A stiff chain model: Monte Carlo calculations

We are interested in the probability distribution function $P(r)$ of the distances $r = |\mathbf{r}_1 - \mathbf{r}_0|$, where $\mathbf{r}_0$ and $\mathbf{r}_1$ are the positions of the initial and final bead of the chain, i.e. the two telomeres TEL1 and TEL2; see figure 1. Since the two arms are constrained to the sphere, known analytical formulae for $P(r)$ of a free chain cannot be applied. The results for a stiff rod model and a freely jointed chain model [3] with two different bond lengths are shown in figure 2.

These simple simulations show that increasing the flexibility of a chromosome has dramatic consequences on the distribution of its end-to-end distance, allowing the two ends to get closer.

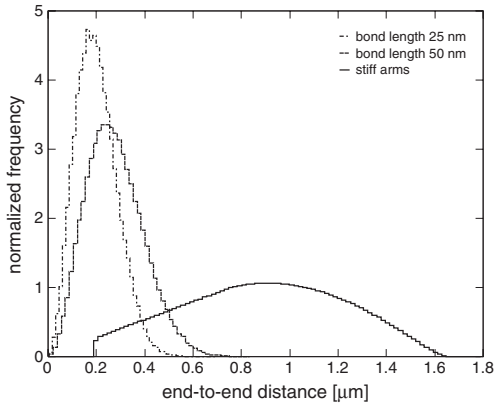

Figure 2. $P(r)$ for a freely jointed chain (see figure 1, [3]) with bond lengths b of 25 and 50 nm. The lengths of the arms used were 1139 and 938 nm, corresponding to chromosome 6 (genomic length in bp divided by 130 bp/nm [1]). The distribution for a model where the chromosome arms are represented as stiff rods is shown for comparison.

While the freely jointed chain model gives a good first approximation of the effect of increasing polymer flexibility, its validity is restricted to chains that are longer than ten statistical segments, which is not the case for yeast chromosomes 3 and 6. For a quantitative comparison of the model with experimental data, we therefore used the more detailed wormlike chain model [3]. The code of the simulation program is based upon the previously described Monte Carlo and Brownian dynamics simulation package *corchy++* [4]. A chain was modelled by a linear sequence of segments connected by flexible joints; the bending energy at the ith joint is given by

$$\frac{E_i}{k_\mathrm{B}T} = \alpha\beta_i^2 \tag{1}$$

where β_i is the joint angle.

The bending rigidity parameter α is directly related to the persistence length L_p [4]. For a free polymer, L_p may be directly related to the mean squared end-to-end distance of the chain (see equation (2)), but for a confined chain this relation is not valid.

Using optimized *in situ* hybridization and live imaging techniques to measure the average end-to-end separation of short intervals of nonrepetitive chromatin, we have previously [1] estimated that the persistence length of interphase chromatin in budding yeast is in the range 170–220 nm by fitting the data to the Kratky–Porod equation [3] for a chain with contour length L_c, persistence length L_p and end-to-end distance r:

$$\langle r^2\rangle = 2L_\mathrm{p}^2 \cdot \left(\mathrm{e}^{-\frac{L_\mathrm{c}}{L_\mathrm{p}}} + \frac{L_\mathrm{c}}{L_\mathrm{p}} - 1\right). \tag{2}$$

Here, we used the same approach to determine the effective persistence length of the simulated chains (see figure 3). For a free chain the data are perfectly consistent with equation (2), but when confining the chain to the nuclear volume there is an agreement only for short subchains. A fit of the Kratky–Porod formula to the data with $d < 400$ nm shows that the contour length given as a parameter for the simulation is well reproduced (with an error of less than 3%), but that the persistence length obtained from the fit is reduced by about 15% as a result of confinement. For the following simulations we chose the rigidity parameter such that the effective persistence length was 200 nm, to match the experimentally determined value [1].

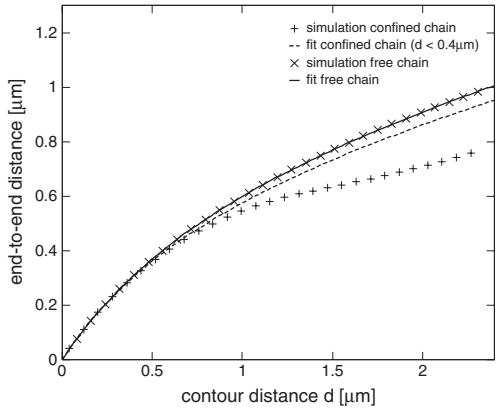

Figure 3. Fit of the square root of the Kratky–Porod formula (equation (2)) to $\sqrt{\langle r^2 \rangle}$ for subchains of contour length d, where r is the end-to-end distance of the subchain. For a free chain the data correspond very well to equation (2), but for a confined chain there is an agreement only for small d.

In the model, the elastic chain is composed of a succession of beads and segments that are represented respectively by balls and cylinders of 30 nm radius and a hard core excluded volume interaction is applied. The centromere bead can be fixed completely or attached elastically to the spindle pole body. Both the excluded volume interaction and the movement of the centromere (± 0.3 μm) had only minor effects on the end-to-end distance distribution (data not shown).

3. Biological applications

We compared the end-to-end distance distributions from the simulations of chromosome 3 and 6 with those obtained from experiments in wild type (wt) yeast cells. The telomeres of both chromosomes were tagged with naturally fluorescent proteins by inserting lac^{op} and tet^{op} arrays in subtelomeric regions [1]. Images of intact yeast cells were acquired in 3D essentially as described in [1], taking two-colour image stacks of 16 planes of 0.2 μm intervals along the z-axis on a ZEISS LSM510 confocal microscope. Distributions of distances are plotted by 0.25 ± 0.125 μm categories. Telomeres have a propensity to locate near the nuclear periphery, which we refer to as peripheral anchoring. However, telomere anchoring is dynamic and allows the telomeres to slide along the nuclear envelope within a certain perimeter [5]. To study the effect of telomeric constraint near the nuclear periphery we also used data from mutant cells which lack either the yKu70 protein or the Sir4 protein which both are implicated in the anchoring of yeast telomeres [2, 5].

Figure 4 shows the distribution of the 3D distances between the telomeres of chromosome 6 and 3 in intact, living yeast nuclei [2] cultivated in glucose-containing medium. In both cases the telomere–telomere distance in wild type cells, in which both telomeres are anchored at the nuclear envelope [2, 5], were substantially smaller than for the simulated chains which were not attached to the periphery. Although the preferred peripheral location of telomere 6L is compromised in a *sir4* mutant, the absence of Sir4p did not result in a significant change of the telomere–telomere distance. In contrast, the deletion of *YKU70*, which leads to a random position of telomere 6R in the nucleus, significantly increased the distance between the two telomeres, although this distance is still slightly smaller than in the simulations.

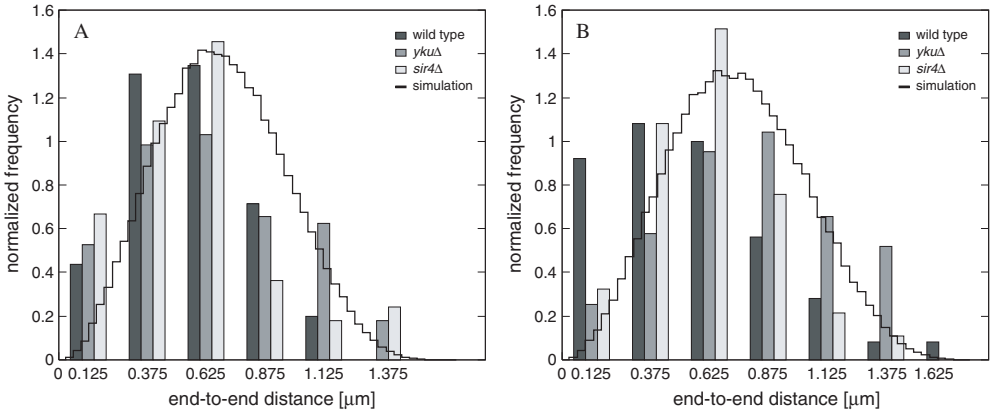

Figure 4. End-to-end distance distribution for chromosomes 6 (A) and 3 (B) in wild type (wt), *yku70*Δ and *sir4*Δ strains in comparison to the simulated data for free chains. The histograms for the simulation data were each calculated from 150 000 independent conformations. (A) The difference between the wt and the simulated distributions is highly significant ($p < 10^{-9}$ in a t-test). The distances in *yku70*Δ are significantly larger than in wt ($p < 0.004$) and close to the prediction ($p < 0.03$) while the distribution for *sir4*Δ does not differ significantly from wt. (B) Again the wt distances are substantially smaller than simulated ($p < 10^{-6}$) and the absence of yKu70p leads to a strong increase of the end-to-end distance which becomes larger than predicted ($p < 0.008$).

The mutation of *YKU70* also caused a clear increase in the end-to-end distance of chromosome 3, which became larger than the simulated distance between the ends of free chains. Again the mutation of *SIR4* had no significant effect on this distance distribution. However, for chromosome 3, in contrast to chromosome 6, both telomeres are released in a *sir4* mutant whereas the absence of yKu70p increases the anchoring of one of the telomeres such that both telomeres are now well anchored [6]. The distribution characteristics of the experimental and the simulated data are summarized in table 1.

The small distances we observed between the telomeres of chromosomes 3 and 6 are characteristic of telomeres belonging to the same chromosome since the distance between two unrelated, anchored telomeres was larger than our simulations would predict for untethered telomeres (figure 5).

To investigate the impact of telomere anchoring on the telomere–telomere distance we simulated the end-to-end distances in the case where the movement of one or two ends of the chromosome is restricted to the nuclear periphery. In order to accomplish that, the following two Monte Carlo steps were used after generating a conformation with peripheral telomeres.

(i) Internal rotation. A subchain is rotated around the axis connecting the two terminal beads. This does not affect telomere position.
(ii) Tail rotation. One part of a chromosome arm beginning at a randomly chosen bead is rotated around the nuclear diameter through this bead. Such a rotation preserves distances from the nuclear centre and therefore moves the chain end to the periphery.

Figure 6 shows the simulated end-to-end distance distribution of chromosome 6 for the four possible scenarios. The simulations revealed that the anchoring of one telomere increased the telomere–telomere distance. In the case where both telomeres were tethered the distance between them increased even further. As expected, the effects of anchoring on the simulated distances between the telomeres of chromosome 3 are the same (table 1).

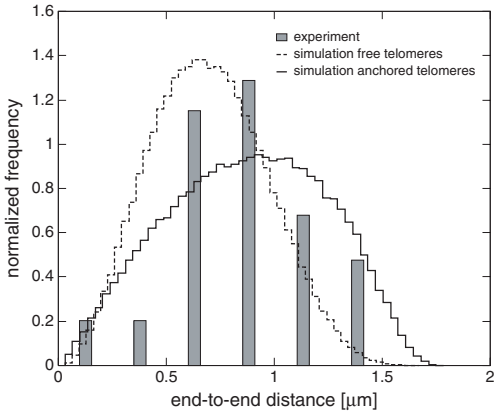

Figure 5. Distance distribution for telomeres 5L and 14R in wild type yeast compared to the simulated distance between two chromosome arms of the same lengths as 5L and 14R modelled using a single completely flexible centromere and either anchored or nonanchored ends. The bending energy for the two independent arms at the centromeric bead was set to zero, such that the two arms can move independently. Here, in contrast to the results for chromosomes 3 and 6, the distances in the simulation without anchoring were significantly smaller than the experimental telomere–telomere distances ($p < 10^{-5}$ in a t-test) while the mean of the simulated data for anchored telomeres agrees with the mean of the experimental distance distribution ($p > 0.2$).

Table 1. Sample size n, mean r and standard deviation σ for the experimental and simulated distributions.

Telomeres	Experiment/simulation	n	r (μm)	σ (μm)
6R 6L wt	Experiment	153	0.558	0.259
6R 6L *yku70*Δ	Experiment	192	0.650	0.351
6R 6L *sir4*Δ	Experiment	66	0.564	0.328
6R free 6L free	Simulation	150 000	0.688	0.263
6R anchored 6L free	Simulation	150 000	0.835	0.275
6R free 6L anchored	Simulation	150 000	0.821	0.275
6R anchored 6L anchored	Simulation	150 000	0.871	0.346
3R 3L wt	Experiment	56	0.548	0.358
3R 3L *yku70*Δ	Experiment	108	0.801	0.354
3R 3L *sir4*Δ	Experiment	37	0.611	0.282
3R free 3L free	Simulation	150 000	0.736	0.281
3R anchored 3L free	Simulation	150 000	0.874	0.298
3R free 3L anchored	Simulation	150 000	0.900	0.297
3R anchored 3L anchored	Simulation	150 000	0.946	0.378
5L 14R wt	Experiment	58	0.838	0.311
5L free 14R free	Simulation	150 000	0.697	0.267
5L anchored 14R anchored	Simulation	150 000	0.875	0.360

In addition, we have shown that the simulated data for two independently anchored telomeres agree well with the mean distance between two unrelated but well anchored telomeres of chromosome arms of similar length (figure 5). These distances are significantly greater than those monitored for the two telomeres of chromosomes 3 and 6. We conclude therefore that telomeric anchoring cannot account for the small telomere–telomere distances that we observe in the experiments for chromosomes 3 and 6.

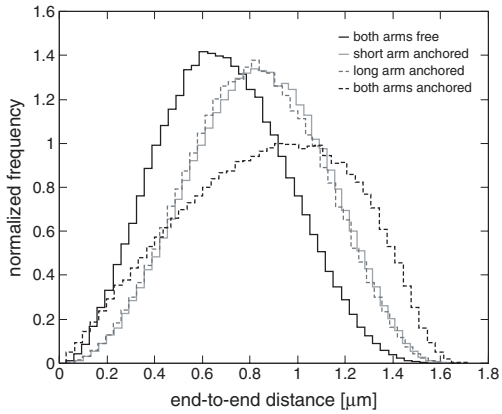

Figure 6. Simulated end-to-end distance distribution for chromosome 6 with 0, 1 and 2 telomeres anchored to the periphery. Tethering of one telomere increased the end-to-end distance. This effect was amplified by anchoring of the second one. Thus telomere anchoring cannot account for the small experimental distances observed between the telomeres of chromosomes 3 and 6.

4. Conclusions

We describe a theoretical treatment to analyse the extension of flexible chromatin fibres of defined diameter in constrained geometries. We have analysed the effect of the flexibility of the modelled fibre and the degree of freedom as modelled by 0, 1 or 2 points of anchorage to the periphery of the confining sphere.

We have applied the developed formalism to analyse data obtained in living yeast cells under varying biological conditions (absence of confining factors as identified by the proteins Sir4 and yKu70 [5] by mutagenesis).

The analysis indicates that intrinsic properties of the chromatin fibre, in particular its elastic properties and flexibility, influence the juxtaposition of the telomeric ends of chromosomes, modelled here as polymer fibres. Yet, as measured in yeast cells, the telomeres of chromosomes 3 and 6 came even closer together than the parameters of constraint imposed on the simulations would predict. Importantly, simulations predicted greater separation between anchored than between free telomeres. This general trend in distance variation was also observed experimentally: the distance between the two completely free telomeres of chromosome 3 in a *sir4* mutant was smaller than the distance between two anchored telomeres in a *yku70* mutant. However, in wild type yeast where both telomeres assume a preferentially peripheral position, the distance between them was even smaller than in the *sir4* mutant and also smaller than predicted for two completely free telomeres. Similarly, the telomeres of chromosome 6 were very close to each other: in contrast to the simulations, the distance in wild type cells where both telomeres are anchored was smaller than the distance observed in mutant strains where one telomere is free. Two mutually non-exclusive mechanisms might lead to this exceptional degree of juxtaposition. One cause could be a direct interaction between the chromosomal ends. Alternatively, the mechanics of mitosis might result in the two ends of a single chromosome being close together as an interphase nucleus forms. A restricted mobility of telomeres in interphase would then account for the fact that they do not separate from each other.

In the mutants examined here the end-to-end distance between the telomeres of chromosome 6 remained substantially smaller than simulated for one free telomere, which is the situation created by the mutation of either *YKU70* or *SIR4*. If this juxtaposition were due to

affinity between telomeric ends, then we must conclude that the loss of either Sir4p or yKu70p does not fully compromise the interaction. This force then clearly overrides the separating tendency imposed by anchoring.

In the simulations we assumed that anchored telomeres can freely explore any point along the nuclear envelope. This, however, is a simplification and recent analysis of telomere movement in living cells over a defined time period [7, 8] demonstrated that the movement of telomeres 3R and 6R is limited to subzones of the nucleus. Given that telomere mobility is limited, it is possible that telomere juxtaposition in interphase is also influenced by the spatial arrangement resulting from mitosis. As the centromeres are pulled to opposite poles by the mitotic spindle, the telomeres trail behind and occupy a more limited nuclear space than theoretically predicted for random polymer chains. If this were to specifically favour the juxtaposition of telomeres belonging to one chromosome as the cell enters G1, then the limited mobility attributed to telomeres might perpetuate this arrangement. It should be noted, however, that telomeres monitored by time-lapse microscopy did not appear to get closer together in mitosis, but rather seemed to separate more (KB, unpublished results). Nonetheless, the mechanical parameters of mitotic division may contribute to telomere position.

In conclusion, more than one factor is likely to influence the end-to-end distances between telomeres, which were far smaller for yeast chromosomes 3 and 6 than expected for random polymer chains. Part of this effect undoubtedly arises from protein–protein interactions. However, the Rabl-like conformation that occurs during anaphase might also increase the probability that telomeres of the same chromosome are close to each other. It is tempting to speculate that the juxtaposition of telomeres belonging to the same chromosome facilitates nuclear processes such as recombination or chromosome segregation, yet further experiments are needed to elucidate the mechanisms involved. The large increase in telomere–telomere distances observed in *yku70* mutants suggests a role for yKu70p, a protein involved in DNA repair, recombination and telomere structure, in the interaction between the two telomeres of one chromosome. It will now be interesting to identify additional factors implicated in the folding of chromosomes through telomere interaction.

Acknowledgments

We thank J H Maddocks and A Stasiak for insightful discussions. LRG and SMG are supported by SNF grant 3100-061605, NCCR Frontiers in Genetics and the Novartis Research Foundation. The research of AR was sponsored by SNF Grants No 3152-68151.02 and 3100A0-103962. JL was supported by DFG grant La 500/8.

KB is funded by La Ligue contre le Cancer and by the Université Paul Sabatier.

References

[1] Bystricky K, Heun P, Gehlen L, Langowski J and Gasser S M 2004 *Proc. Natl Acad. Sci. USA* **101** 16495
[2] Bystricky K, Laroche Th, van Houwe G, Blaszczyk M and Gasser S M 2005 *J. Cell Biol.* **168** 375
[3] Doi M and Edwards S F 1986 *The Theory of Polymer Dynamics* (Oxford: Oxford University Press)
[4] Klenin K, Merlitz H and Langowski J 1998 *Biophys. J.* **74** 780
[5] Hediger F, Neumann F R, Van Houwe G, Dubrana K and Gasser S M 2002 *Curr. Biol.* **12** 2076
[6] Bystricky K, Van Attikum H and Gasser S M 2005 in preparation
[7] Rosa A, Maddocks J H, Neumann F R, Gasser S M and Stasiak A 2005 *Biophys. J.* at press
[8] Heun P, Laroche Th, Shimada K, Furrer P and Gasser S M 2001 *Science* **294** 2181